

The gluon condensation: a secret hidden in HESSs J1826-130, J1641-463 and J1741-302

Jianhong Ruan, Zechun Zheng and Wei Zhu*

Department of Physics, East China Normal University, Shanghai 200241, China

Abstract

The gluon condensation predicted by a nonlinear QCD evolution equation can naturally explain the typical broken power law in the γ -ray spectra at very high energy. This result is used to perfect the incomplete spectra HESSs J1826-130, J1641-463 and J1741-302. We show the distinctive characteristics of these spectra, which are different from the other spectra models and they can be tested by further observations.

keywords: Gluon condensation: Astroparticle physics: Gamma rays:

1 Introduction

The discovery of very high energy (VHE) gamma-ray sources around the galactic centre opens a new era for studies of the cosmic ray acceleration and transformation. There are several VHE sources, for example, HESSs J1826-130 [1], J1641-463 [2] and J1741-302 [3] present a typical power law with the hard photon index $\Gamma_\gamma \sim 2$ in a broad energy range from several hundred GeV to beyond 10 TeV. Besides, all of them are tagged as unidentified sources and located near other bright VHE sources. Although many works speculated the possible origins of these VHE gamma-ray spectra, their nature is still open. Especially, where and how cosmic rays are accelerated to reach and beyond the necessary PeV energies in our galaxy and in which mechanism the kinetic energy of initial particles (protons or electrons) converts into photons, which can be described by the power-law.

*Corresponding author, E-mail: wzhu@phy.ecnu.edu.cn

An important obstacle is that we lack the extension of the above spectra in the GeV-energy region, and an incomplete spectrum cannot provide the correct information about these sources.

We have pointed out that the hadronic framework considering the gluon condensation (GC) effect may provide a typical broken power in the VHE gamma ray spectra [4-6]. Let us consider the hadronic processes $pp \rightarrow \pi^0$ and $\pi^0 \rightarrow 2\gamma$. The secondary particles (mostly pions) in the $p-p$ collisions are produced by kinetic energy of the protons through the gluons. The gluon distributions in the proton are described by the QCD evolution equations. At very high energy these equations should contain the BFKL singularity both in its linear and nonlinear parts, which is caused by the random walk of the gluons on the transverse momentum space (e.g. [7]). After regularization in the quantum field theory, the evolution equation appears a rapidly chaotic oscillation at a critical momentum $(x_c, k_{t,c})$ (x is the Bjorken variable and k_t is the transverse momentum of gluon), which forms a pair of strong shadowing and antishadowing at every evolution step. They squeeze the gluons at small x to a narrow phase space. This is the gluon condensation (GC).

The GC would change the γ -ray spectra in the traditional hadronic model and presents a special structure, provided the GC-threshold E_{p-p}^{GC} enters the observable energy region. As we will show in equation (2.10) at Sec. 2, these gamma-ray spectra present the typical broken power law with a variable cut-off factor, where the distribution at $E_\gamma > E_\pi^{GC}$ coincides perfectly with the observed spectra of HESSs J1641-463, J1826-130 and J1741-302. In particular, the GC effect decreases the number of free parameters and reduces the uncertainty when we expand the observed spectra toward GeV-energy range.

We will give a brief introduction about the GC model at section 2. The detail derivations can be found in the relating references. In the following sections 3-5 we discuss the γ -spectra of HESSs J1826-130, J1641-463 and J1741-302. We find that the prediction

of the GC model and the characteristics of these spectra are coincident. Referring to the complete VHE γ -ray spectra of neighboring HESS J1825-137 and HESS J1640-465, we determine the values of parameter β_γ for HESSs J1826-130, 1641-463 and J1741-302. Thus we can expend the observed incomplete spectra to GeV energies in the GC model. Section 6 is discussions and summary. The predicted VHE γ -spectra by the GC model show their characteristics, which may be confirmed by further improved observations.

2 The GC model

The flux of high energy gamma ray at hadronic processes $p + p \rightarrow \pi^0 \rightarrow 2\gamma$ in the laboratory frame reads [8-11]

$$\begin{aligned} \Phi_\gamma(E_\gamma) = C_\gamma \left(\frac{E_\gamma}{1GeV} \right)^{-\beta_\gamma} \int_{E_\pi^{min}}^{E_\pi^{max}} dE_\pi \left(\frac{E_p}{1GeV} \right)^{-\beta_p} \\ \times N_\pi(E_p, E_\pi) \frac{d\omega_{\pi-\gamma}(E_\pi, E_\gamma)}{dE_\gamma}, \end{aligned} \quad (2.1)$$

where the spectral index β_γ denotes the propagating loss of gamma-rays inside the source. The accelerated protons obey a power law $N_p \sim E_p^{-\beta_p}$ with the integrated index β_p , or equivalently, in a differential form $dN_p/dE_p \sim E_p^{-\Gamma_p}$, where $\Gamma_p = \beta_p + 1$. C_γ incorporates the kinematic factor with the flux dimension and the percentage of $\pi^0 \rightarrow 2\gamma$. The normalized spectrum for $\pi^0 \rightarrow 2\gamma$ is

$$\frac{d\omega_{\pi-\gamma}(E_\pi, E_\gamma)}{dE_\gamma} = \frac{2}{\beta_\pi E_\pi} H[E_\gamma; \frac{1}{2}E_\pi(1 - \beta_\pi), \frac{1}{2}E_\pi(1 + \beta_\pi)], \quad (2.2)$$

where $H(x; a, b) = 1$ if $a \leq x \leq b$, and $H(x; a, b) = 0$ otherwise, $\beta_\pi \sim 1$. Usually, the relations among N_π , E_π and E_p are very complicated and they are determined by using the limited experimental data. However, we show that the GC effect simplifies the above relations and gives a special energy spectrum.

Because large amounts of meson yields require more gluons in inelastic pp collisions, we assume that a huge number of gluons at the central region due to the GC effect may create the maximum number N_π of pions, which take up all available kinetic energy if we neglect other secondary particles. One can get the following characteristic distributions in the GeV unit

$$\ln N_\pi = 0.5 \ln E_p + a, \quad \ln N_\pi = \ln E_\pi + b, \quad (2.3)$$

$$\text{where } E_\pi \in [E_\pi^{GC}, E_\pi^{max}],$$

and

$$a \equiv 0.5 \ln(2m_p) - \ln m_\pi + \ln K, \quad b \equiv \ln(2m_p) - 2 \ln m_\pi + \ln K, \quad (2.4)$$

$K \simeq 0.5$ is the inelasticity.

Setting equations (2.2)-(2.4) to equation (2.1), we directly get the gamma ray spectrum due to the GC effect.

$$E_\gamma^2 \Phi_\gamma^{GC}(E_\gamma) = \begin{cases} \frac{2e^b C_\gamma}{2\beta_p - 1} (E_\pi^{GC})^3 \left(\frac{E_\gamma}{E_\pi^{GC}} \right)^{-\beta_\gamma + 2} & \text{if } E_\gamma \leq E_\pi^{GC}, \\ \frac{2e^b C_\gamma}{2\beta_p - 1} (E_\pi^{GC})^3 \left(\frac{E_\gamma}{E_\pi^{GC}} \right)^{-\beta_\gamma - 2\beta_p + 3} & \text{if } E_\gamma > E_\pi^{GC}. \end{cases} \quad (2.5)$$

Surprisingly it is a naturally broken power law. Note that the power law at $E_\gamma > E_\pi^{GC}$ is valid if equation (2.3) is held, while the power law at $E_\gamma < E_\pi^{GC}$ is irrelevant to whether equation (2.3) is maintained, provided the number of secondary particles increases rapidly beginning at $E_\gamma = E_\pi^{GC}$.

We turn to discuss the second characteristics of the GC effect in the VHE spectra. Figure 1 is a schematic diagram for the inclusive gluon rapidity distribution with the GC effect at the $p - p$ collision, which is taken from [6]. One can find that the GC effect

begins work if the position of the GC peak locals at $y_{max} = \ln(\sqrt{s_{p-p}^{GC}}/\underline{k}_c)$, thus

$$x_c = \frac{\underline{k}_c}{\sqrt{s_{p-p}^{GC}}} e^{-y_{max}} \simeq \frac{\underline{k}_c^2}{s_{p-p}^{GC}}. \quad (2.6)$$

Combining $\sqrt{s_{p-p}} = \sqrt{2m_p E_p}$ and equation (2.3), we have

$$E_\pi^{GC} = \exp \left(0.5 \ln \frac{\underline{k}_c^2}{2m_p x_c} - (b - a) \right). \quad (2.7)$$

On the other hand, the cross section of $p - p$ collision disappears if the position of the gluon density peak moves to the rapidity center $y = 0$, i.e., at

$$x_c = \frac{\underline{k}_c}{\sqrt{s_{p-p}^{max}}} e^{y=0}, \quad (2.8)$$

or at

$$\begin{aligned} E_\pi^{max} &= \exp \left(0.5 \ln \frac{\underline{k}_c^2}{2m_p x_c^2} - (b - a) \right) = \frac{E_\pi^{GC}}{\sqrt{x_c}} \\ &= e^{b-a} \sqrt{\frac{2m_p}{\underline{k}_c^2}} (E_\pi^{GC})^2 = 14 (E_\pi^{GC})^2. \end{aligned} \quad (2.9)$$

However, figure 1 shows that the platform is shrinking with increasing energy rather than expanding, since lots of soft gluons enter the interaction range early due to the condensation. It implies that the suppression of Φ_γ occurs before E_π^{max} . Therefore we add a cut-off factor in equation (2.5), i.e.,

$$E_\gamma^2 \Phi_\gamma^{GC}(E_\gamma) = \begin{cases} \frac{2e^b C_\gamma}{2\beta_p - 1} (E_\pi^{GC})^3 \left(\frac{E_\gamma}{E_\pi^{GC}} \right)^{-\beta_\gamma + 2} & \text{if } E_\gamma \leq E_\pi^{GC}, \\ \frac{2e^b C_\gamma}{2\beta_p - 1} (E_\pi^{GC})^3 \left(\frac{E_\gamma}{E_\pi^{GC}} \right)^{-\beta_\gamma - 2\beta_p + 3} & \text{if } E_\pi^{GC} < E_\gamma < E_\pi^{cut}, \\ \frac{2e^b C_\gamma}{2\beta_p - 1} (E_\pi^{GC})^3 \left(\frac{E_\gamma}{E_\pi^{GC}} \right)^{-\beta_\gamma - 2\beta_p + 3} \exp \left(-\frac{E_\gamma}{E_\pi^{cut}} + 1 \right) & \text{if } E_\gamma \geq E_\pi^{cut}, \end{cases}, \quad (2.10)$$

or

$$\Phi_{\gamma}^{GC}(E_{\gamma}) \equiv \begin{cases} \Phi_0 \left(\frac{E_{\gamma}}{E_{\pi}^{GC}} \right)^{-\Gamma_1} & \text{if } E_{\gamma} \leq E_{\pi}^{GC}, \\ \Phi_0 \left(\frac{E_{\gamma}}{E_{\pi}^{GC}} \right)^{-\Gamma_2} & \text{if } E_{\pi}^{GC} < E_{\gamma} < E_{\pi}^{cut}, \\ \Phi_0 \left(\frac{E_{\gamma}}{E_{\pi}^{GC}} \right)^{-\Gamma_2} \exp \left(-\frac{E_{\gamma}}{E_{\pi}^{cut}} + 1 \right), & \text{if } E_{\gamma} \geq E_{\pi}^{cut}, \end{cases} \quad (2.11)$$

where

$$E_{\pi}^{cut} = \alpha E_{\pi}^{max} \quad (2.12)$$

and $\alpha < 1$. Note that the suppressed factor $\exp(-E_{\gamma}/E_{\pi}^{cut} + 1)$ works beginning at E_{π}^{cut} rather than at E_{π}^{GC} .

Comparing with the mathematic parameterized form of the broken power law, the parameters of the GC model have specific physical meaning and inner connection. Thus, we can use the GC model to extend the observed HESS spectra to the GeV-energy range and expose the nature behind the spectra as we will show them in the following examples.

3 HESS J1826-130

J1826-130 is an unidentified hard spectrum source discovered by HESS along the Galactic plane. The source had been previously hidden in the extended tail of emission from the nearby bright source HESS J1825-137 [12]. HESS J1826-130 shows a relative hard gamma-ray spectrum. Obviously this present spectrum is incomplete. Let us to perfect it using the GC model. Our logical reasoning is as follows.

(i) Using quation (2.11) at $E_{\gamma} > E_{\pi}^{GC}$ to fit the HESS J1826-130 data, one can find that a single power law with $\Gamma_{\gamma} \sim 2$ extends up to 14 TeV, then appears a cut-off factor (see figure 2). According to equations (2.9) and (2.12), we have the breaking location

$E_{\pi}^{GC} = 100 \text{ GeV}$, where we take $\alpha = 0.1$.

(ii) We turn to HESS J1825-137 to look for the information relating HESS J1826-130. HESS J1825-137 combining the Fermi-LAT data has a complete gamma ray spectrum in $10 \text{ GeV} - 10 \text{ TeV}$. We find that the spectrum can also be fitted by equation (2.10). The parameters are $\beta_{\gamma} = 1.69$, $\beta_p = 0.91$, $C_{\gamma} = 3.5 \times 10^{-12} [\text{TeV}^{-2} \text{cm}^{-2} \text{s}^{-1}]$ and $E_{\pi}^{GC} = 0.115 \text{ TeV}$. Using equations (2.9) and (2.12) we have $E_{\pi}^{cut} = 18 \text{ TeV}$. We noticed that the spectrum of HESS J1825-137 was explained by using a leptonic model [13]. For comparison, we present it in figure 3 (dashed curve). Note that the parameter β_p in the GC model is determined by the accelerate mechanism of the protons. Therefore, we assume that two close sources have a same value of β_p . Thus, we have

$$-\beta_{\gamma} - 2 \times 0.91 + 1 = -2, \quad (3.1)$$

for HESS J1826-130. Now we can predict a complete spectrum of J1826-130 in figure 4 since we have $\beta_{\gamma} = 1.18$.

Why there is no recorded spectrum of HESS J1826-130 at $E_{\gamma} < 100 \text{ GeV}$? We noticed that J1826-1256 is a radio quiet gamma-ray pulsar discovered by Fermi-LAT [14]. Its position is near J1826-130. The spectrum of HESS J1826-1256 at GeV energies is shown in figure 4, it may shadow the spectrum of HESS J1826-130 in the observation and leads an incomplete spectrum.

4 HESS J1641-463

A same program as in the above section is used to discuss HESS J1641-463 [2]. HESS J1641-463 remains unknown by the usual analysis techniques due to confusion with the bright nearby source HESS J1640-465 [15]. No X -ray candidate stands out as a clear association. It tends to the hadronic mechanism, where the emission is produced by

cosmic ray protons colliding with the ambient gas [3]. The data in figure 5 tell us that $\Gamma_2 = 2.07$ and $E_\pi^{cut} = 14 \text{ TeV}$ in equation (2.11) in the GC model. According to equation (2.12), $E_\pi^{GC} = 0.1 \text{ TeV}$.

Then we discuss the relating VHE gamma ray source J1640-465. This spectrum was connected to a hard Fermi-LAT gamma-ray spectrum with photon index $\Gamma_1 \sim 2$ and was explained in the traditional hadronic model [16,17]. However, Yu-Liang Xin et al reanalyze the relating Fermi-LAT data [18] and find that an extended GeV gamma-ray source positionally coincident with J1640-465. Its photon spectrum is described by a power-law with an index of 1.42 ± 0.19 in the energy range of 10-500 GeV, and smoothly connects with the TeV spectrum of HESS J1640-465. We use the same Fermi-LAT data in [18] in the GC model to describe the expanded spectrum of HESS J1640-465. The result is present in figure 6 (solid curve). The parameters are $\beta_\gamma = 1.42$, $\beta_p = 1.04$, $E_\pi^{GC} = 0.1 \text{ TeV}$, and $C_\gamma = 8.7 \times 10^{-13} [\text{TeV}^{-2} \text{cm}^{-2} \text{s}^{-1}]$. For comparison, a description by the leptonic model is also shown in figure 6 (dashed curve).

Assuming the proton beams in HESS J1641-463 and HESS J1640-465 origin from a same accelerator. Thus we take $\beta_p = 1.04$ for HESS J1641-130. One can get $\beta_\gamma = 0.99$. Thus, we have a complete spectrum for J1641-463 in figure 7. The hollow points are the detected pulsed emission of SNR G338.5+0.1 by Fermi-LAT [19]. We add it in figure 7 and indicate that they may cover the extension of the HESS spectrum in GeV energies.

5 HESS J1741-302

A preliminary detection of HESS J1741-302 was early announced by HESS [20]. After that, thanks to the increased amount of high quality VHE data and improved analysis techniques employed, spectrum of HESS J1741-302 can now be characterised in detail [3]. However, the region around HESS J1741-302 is rather complex. A compact radio source

and a variable star are spatially coincident with the position of HESS J1741-302. HESS J1741-302 is not only unidentified but also no plausible counterpart has been found at the high-energy (HE, 0.1-100 GeV) range. We have only an incomplete spectrum as shown in figure 8.

We try use the GC model to expose its nature in a similar way. From the distribution of gamma rays in figure 8. one can read that $-\beta_\gamma - 2\beta_p + 1 = -\Gamma_2 = -2.3$. On the other hand, $E_\pi^{cut} \simeq 14 \text{ TeV}$ corresponding to $E_\pi^{GC} = 0.1 \text{ TeV}$.

We have got $\beta_p = 0.91$ for J1826-130 and 1.02 for J1641-463. They differ by 0.11. On the other hand, the measured value of Γ_2 for these two sources has an error 0.11 ± 0.20 . Therefore, we assume that the above three VHE gamma rays origin from a similar proton accelerate mechanism in our Galaxy and we take approximately $\beta_p \simeq 1$ for J1741-302. Thus, a complete VHE gamma ray spectrum can be predicted in figure 9.

An investigation of the Fermi LAT data has revealed a new HE source Fermi J1740.1-3013 [21], which is $\sim 0.3^\circ$ offset from the best fit position of HESS J1741-302. We draw it in figure 9 and find that the spectrum of HESS J1741-302 at GeV energies may be covered or mixed by this new source.

6 Discussions and Summary

Equation (2.11) describes a sharp broken power with a cut-off factor at $E_\pi^{cut} \gg E_\pi^{GC}$. As figures 2, 5 and 8 show that the spectra keep a beautiful line at $E_\pi^{GC} < E_\gamma < E_\pi^{cut}$ on the double logarithmic coordinate system. It is different from either the leptonic model and the traditional hadronic model. We expect more accurate inspection of observation data.

The spectral hardness is described by the index Γ_2 in equation (2.11), which is determined by two parameters β_γ and β_p in the GC-model. One can find that the spectra of HESS J1826-130 and HESS J1641-463 are harder than that of HESS J1825-137 and HESS

J1640-465. Therefore, we suggest that the formers have a relatively cleaner environment, i.e., a smaller value of β_γ .

Summary, the gluon condensation originating from a nonlinear QCD evolution equation may naturally form the broken power law in the γ -ray spectra at very high energy. This result is used to perfect the incomplete spectra of HESSs J1826-130, J1641-463 and J1741-302. The resulting spectra are different from other models and they can be tested by further observations.

Acknowledgments: This work is supported by the National Natural Science of China (No.11851303).

References

- [1] E.O. Angner, F. Aharonian, P. Bordas, et al., (H.E.S.S. Collaboration), HESS J1826-130: *A Very Hard γ -Ray Spectrum Source in the Galactic Plane*, *AIP Conf. Proc.*, **1792** (2017) 040024 [arXiv:1701.07002].
- [2] A. Abramowski, F. Aharonian, F. Ait Benkhali, et al. (H.E.S.S. Collaboration), *Discovery of the hard spectrum VHE γ -ray source HESS J1641-463*, *Astrophys. J.* **794** (2014) L1 [arXiv:1408.5280].
- [3] H. Abdalla, A. Abramowski, F. Aharonian et al., *HESSJ1741-302: a hidden accelerator in the Galactic plane*, *A&A bf A13* (2018) 612 [arXiv:1711.01350].
- [4] W. Zhu, Z.Q. Shen and J.H. Ruan, *Can a chaotic solution in the QCD evolution equation restrain high-energy collider physics?* *Chin. Phys. Lett.* **25** (2008) 3605 [arXiv:0809.0609].

- [5] W. Zhu, Z.Q. Shen and J.H. Ruan, *The chaotic effects in a nonlinear QCD evolution equation*, *Nucl. Phys.* **B911** (2016) 1 [arViv:1603.04158]
- [6] W. Zhu and J. Lan, *The gluon condensation at high energy hadron collisions*, *Nucl. Phys.* **B916** (2017) 647 [arXiv:1702.02249].
- [7] Y. Kovchegov and E. Levin, *Quantum chromodynamics at high energy*, Cambridge, *Universkty press*, (2012).
- [8] W. Zhu, J.S. Lan and J.H. Ruan, *The gluon condensation in high energy cosmic rays*, *Int. J. Mod. Physics* **E27** (2018) 1850073 [arXiv:1709.03897].
- [9] W. Zhu, P. Liu, J.H. Ruan and F. Wang, *Possible Evidence for the Gluon Condensation Effect in Cosmic Positron and GammaRay Spectra*, *Astrophys. J.* **889** (2020) 127 [arXiv:1912.12842].
- [10] W. Zhu, Z.C. Zheng, P. Liu, L.H. Wan, J.H. Ruan and F. Wang, *Looking for the possible gluon condensation signature in sub-TeV gamma-ray spectra: from active galactic nuclei to gamma ray bursts*, *JCAP* ? (2020) ? [arXiv:2009.01984].
- [11] W. Zhu, P. Liu, J.H. Ruan, R.Q. Wang and F. Wang, *The gluon condensation effect in the cosmic hadron spectra*, *JCAP* **09** (2020) 011 [arXiv:2002.06294].
- [12] F.A. Aharonian, et al., *A possible association of the new VHE gamma-ray source HESS J1825-137 with the pulsar wind nebula G18.0-0.7*, *A&A* **442** (2005) 25 [arXiv:0519304].
- [13] G. Principe, A.M.W. Mitchell, S. Caro?, J. A. Hinton, R.D. Parsons and S. Funk, *Energy dependent morphology of the pulsar wind nebula HESS J1825-137 with Fermi-LAT*, *A&A* **640** (2020) A76 [arViv:2006.11177].

- [14] J. Li, Diego F. Torres, F. Coti Zelati, A. Papitto, M. Kerr and N. Rea, *Theoretically motivated search and detection of non-thermal pulsations from PSRs J1747-2958, J2021+3651 and J1826-1256*, *Astrophys.J.Lett.* **868** (2018) L29 [arXiv:1811.08339].
- [15] F. Aharonian, A.G. Akhperjanian, A.R. Bazer-Bachi, et al. *The H.E.S.S. survey of the Inner Galaxy in vehigh-energy gamma-rays*, *A&A* **636** (2006) 777 [arXiv:0510397].
- [16] M. Lemoine-Goumard, M.-H. Grondin, F. Acero, J. Ballet, H. Laffon, T. Reposeur, *HESS J1640-465 and HESS J1641-463: two intriguing TeV sources in the light of new Fermi LAT observations*, *Astrophys.J.Lett.* **794** (2014) L16 [arXiv:1409.4994].
- [17] L. Supan, A. D. Supanitsky, G. Castelletti, *The environment of the gamma-ray emitting SNR G338.3-0.0: a hadronic interpretation for HESS J1640-465*, *A&A* **589** (2016) A51 [arXiv:1603.05137].
- [18] Y.L. Xin, N.H. Liao, X.L. Guo, Q. Yuan, S.M. Liu¹, Y.Z. Fan and D.M. Wei, *HESS J1640-465-A gamma-ray emitting pulsar wind nebula?* *Astrophys.J.* **867** (2018) 55 [arXiv:1802.03520].
- [19] M. Lemoine-Goumard, M. H. Grondin, F. Acero, J. Ballet, H. Laffon and T. Reposeur, *HESS J1640-465 and HESS J1641-463: Two intriguing TeV sources in the light of new Fermi TAT observations*, *Astrophys.J.Lett.* **94** (2014) L16 [arXiv:1409.4994].
- [20] O. Tibolla, N. Komin, K. Kosack and M. Naumann-Godo, *High energy gamma-ray astronomy*, *AIP Conf. Proc.*, **1085** (2008) 249.
- [21] C. Y. Hui, P. K. H. Yeung, C. W. Ng, L. C. C. Lin, P. H. T. Tam, K. S. Cheng, A. K. H. Kong, D. O. Chernyshov and V. A. Dogiel, *Observing two dark accelerators around*

the Galactic Centre with Fermi Large Area Telescope, *Mon.Not.Roy.Astron.Soc.* **457**

(2016) 4262 [arXiv:1601.06500].

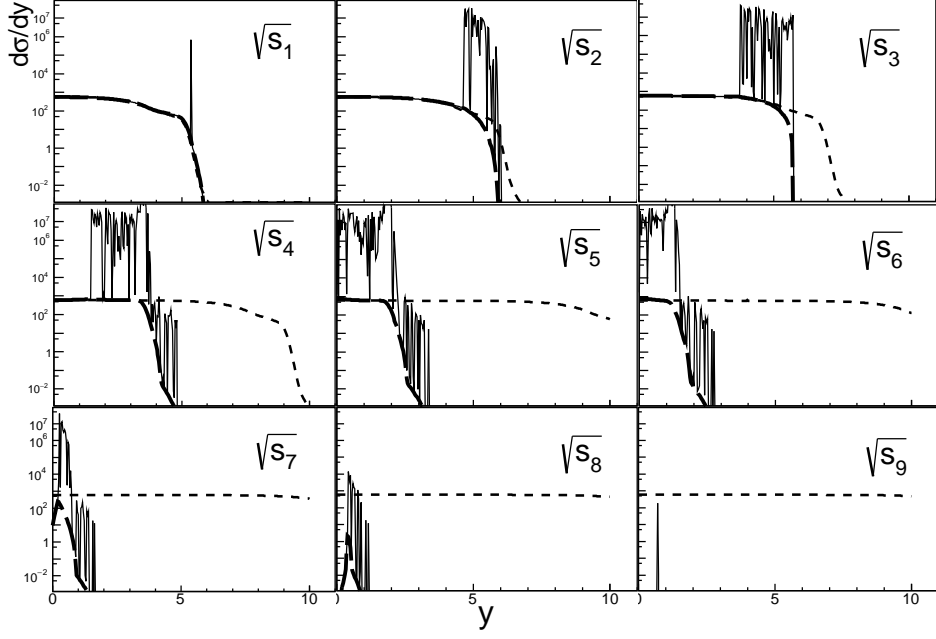


Figure 1: A schematic diagram for the inclusive gluon rapidity distribution at $p - p$ collisions (taking from [6]), where $\sqrt{s_{i+1}} > \sqrt{s_i}$. The results show the large fluctuations are arisen by the GC.

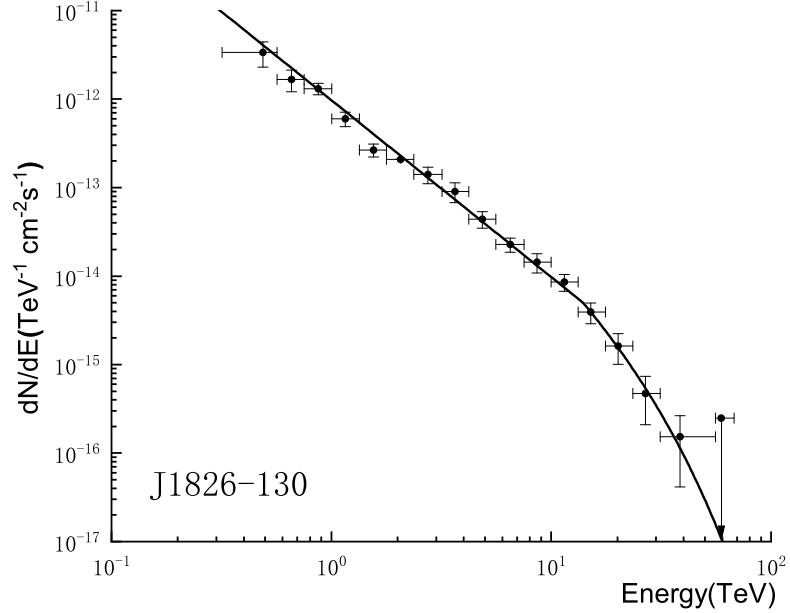


Figure 2: An incomplete VHE γ -ray spectrum of HESS J1826-130. The black data points are the H.E.S.S. measured photon flux [1]. The parameters of the GC model read $\Gamma_2 = 2$ and $E_\pi^{cut} = 18 \text{ TeV}$ in equation (2.11).

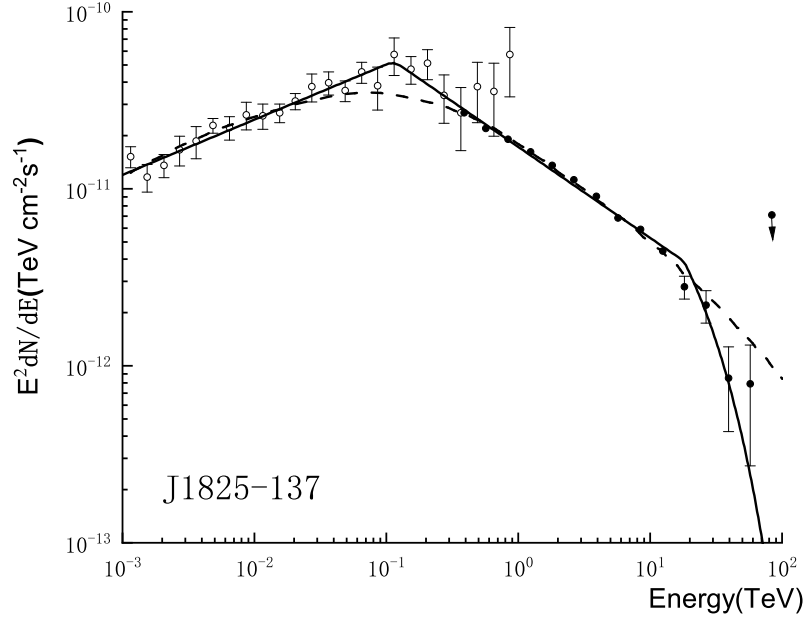


Figure 3: The VHE γ -ray spectrum of HESS J1825-137 (black points) combining the Fermi-LAT data (hollow points) [10]. The solid curve is the GC model fitting, where the parameters in equation (2.10) read $\beta_\gamma = 1.69$, $\beta_p = 0.91$, $C_\gamma = 3.5 \times 10^{-12} [TeV^{-2} cm^{-2} s^{-1}]$, $E_\pi^{GC} = 0.1 TeV$ and $E_\pi^{cut} = 14 TeV$. Note that $\Gamma_2 - \Gamma_1 = 0.82$. The dashed curve is the prediction of a leptonic model [13].

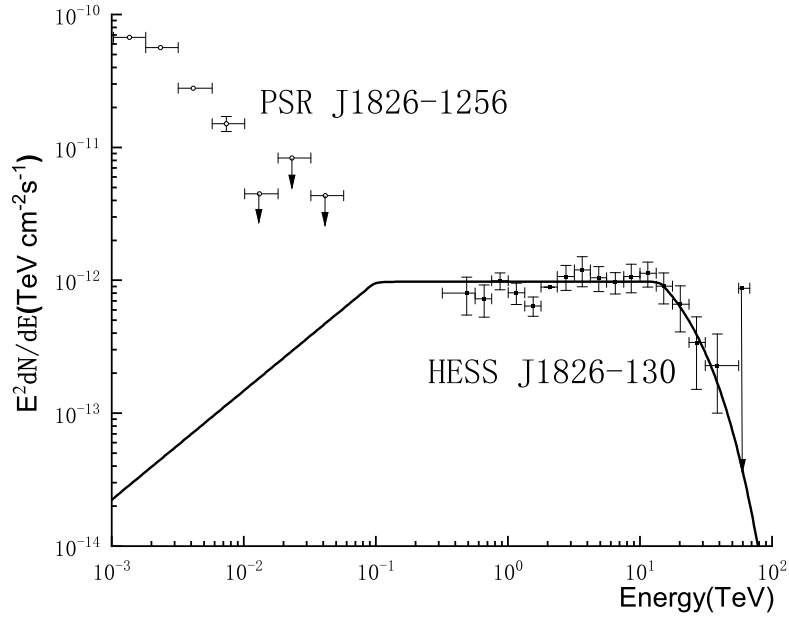


Figure 4: A complete VHE γ -ray spectrum of HESS J1826-130 predicted by the GC model (solid curve). The parameter $\beta_p \equiv 0.91$ is fixed by HESS J1640-465. Using equations (2.10)-(2.12) we have $\beta_\gamma = 1.18$ and $E_\pi^{GC} = 0.1 \text{ TeV}$. C_γ reads $7.8 \times 10^{-14} [\text{TeV}^{-2} \text{cm}^{-2} \text{s}^{-1}]$. or $\Phi_0 = 9.75 \times 10^{-13} [\text{TeV}^{-1} \text{cm}^{-2} \text{s}^{-1}]$. Note that $\Gamma_2 - \Gamma_1 = 0.82$. The hollow points are the data relating to a neighboring PSR J1826-1256 [12], which may shadow the spectrum of HESS J1826-130 at $E_\gamma < 0.1 \text{ TeV}$.

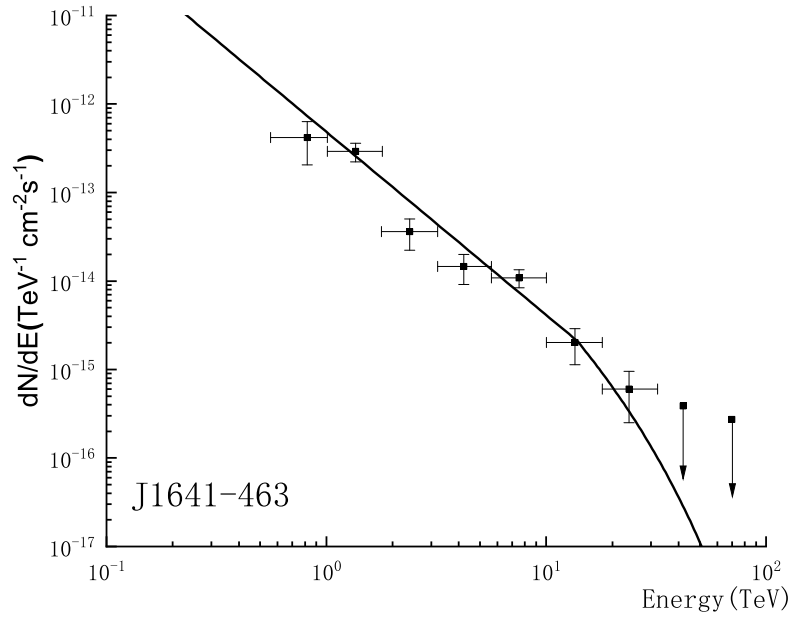


Figure 5: An incomplete VHE γ -ray spectrum of HESS J1641-463 [2]. The black data points are the H.E.S.S. measured photon flux. The parameters of the GC model read $\Gamma_2 = 2.07$ and $E_{\pi}^{cut} = 14 \text{ TeV}$ in equation (2.11).

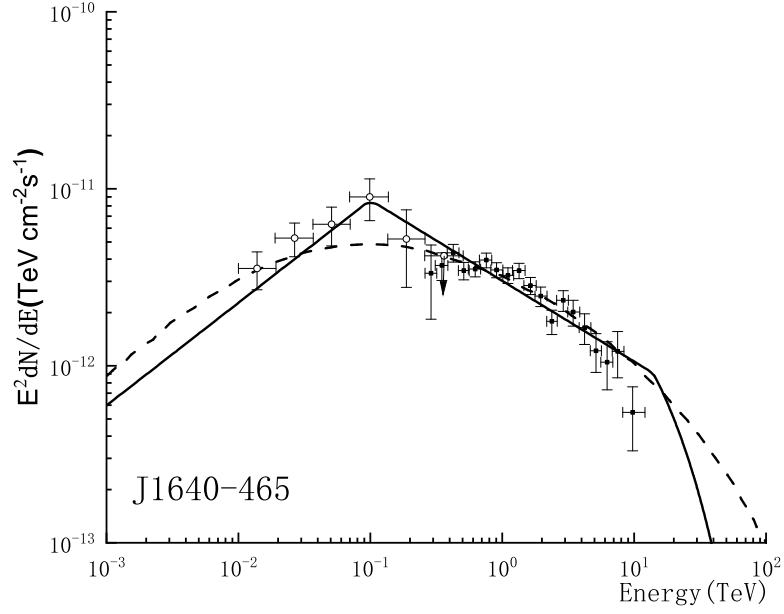


Figure 6: The VHE γ -ray spectrum of HESS J1640-465 (black points) combining the Fermi-LAT data (hollow points) [14]. The solid curve is the GC model fitting, where the parameters in equation (2.10) read $\beta_\gamma = 1.42$, $\beta_p = 1.02$, $C_\gamma = 8.7 \times 10^{-13} [TeV^{-2} cm^{-2} s^{-1}]$, $E_\pi^{GC} = 0.1 TeV$ and $E_\pi^{cut} = 14 TeV$. Note that $\Gamma_2 - \Gamma_1 = 1.04$. The dashed curve is the prediction of a leptonic model [18].

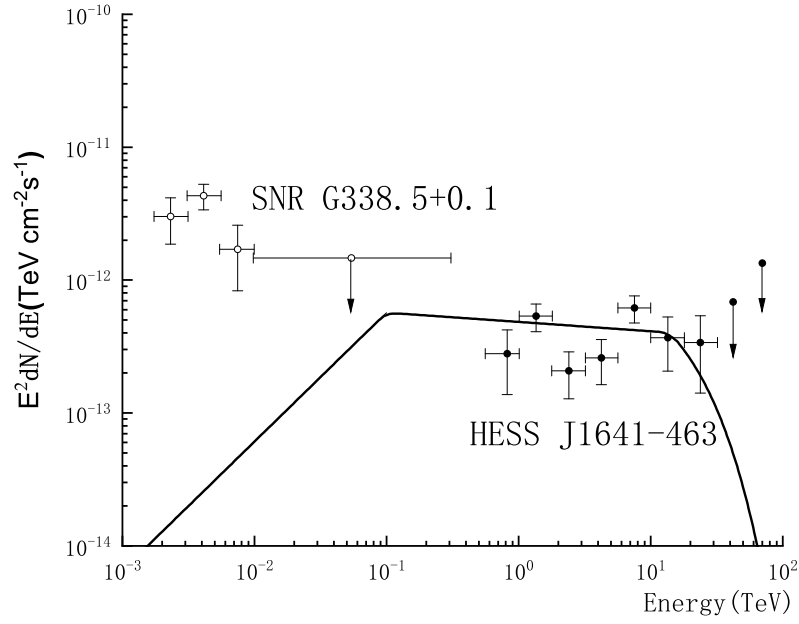


Figure 7: A complete VHE γ -ray spectrum of HESS J1641-463 predicted by the GC model (solid curve). The parameter $\beta_p \equiv 1.02$ is fixed by HESS J1640-465. Using equations (2.10)-(2.12) we have $\beta_\gamma = 1.03$ and $E_\pi^{GC} = 0.1 \text{ TeV}$. C_γ reads $5.7 \times 10^{-14} [\text{TeV}^{-2} \text{cm}^{-2} \text{s}^{-1}]$ or $\Phi_0 = 5.69 \times 10^{-13} [\text{TeV}^{-1} \text{cm}^{-2} \text{s}^{-1}]$. Note that $\Gamma_2 - \Gamma_1 = 1.04$. The hollow points are the data relating to a neighboring SNR G338.5+0.1 [18], which may shadow the spectrum of J1641-463 at $E_\gamma < 0.1 \text{ TeV}$.

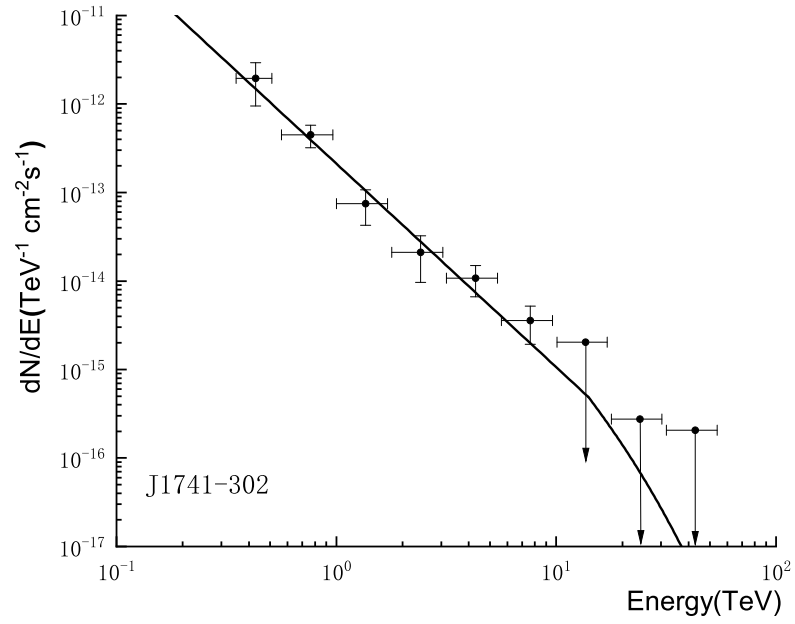


Figure 8: An incomplete VHE γ -ray spectrum of HESS J1741-302 [3]. The black data points are the H.E.S.S. measured photon flux. The parameters of the GC model read $\Gamma_2 = 2.3$ and $E_{\pi}^{cut} = 14 \text{ TeV}$ in equation (2.11).

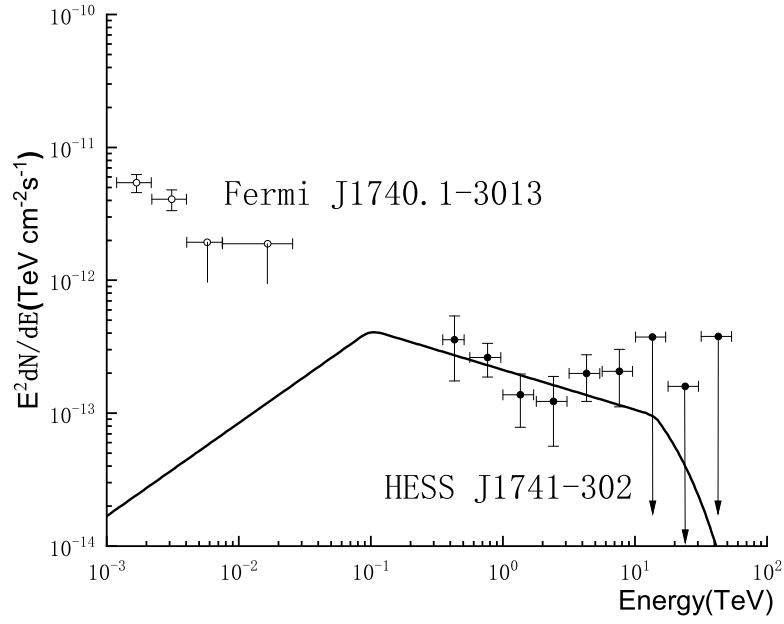


Figure 9: A complete VHE γ -ray spectrum of HESS J1741-302 predicted by the GC model (solid curve). The parameter $\beta_p \equiv 1$, it refers to HESS J1641-463 and HESS J1826-139. Using equations (2.10)-(2.12) we have $\beta_\gamma = 1.3$ and $E_\pi^{GC} = 0.1 \text{ TeV}$. C_γ reads $4.1 \times 10^{-14} [\text{TeV}^{-2} \text{cm}^{-2} \text{s}^{-1}]$ or $\Phi_0 = 4.23 \times 10^{-13} [\text{TeV}^{-1} \text{cm}^{-2} \text{s}^{-1}]$. The hollow points are the data relating to a neighboring Fermi J1740.1-3013 [20], which may shadow the spectrum of J1741-302 at $E_\gamma < 0.1 \text{ TeV}$.